# Supplementary Information

## Degradation of reactive black 5 via Cu(II)/$NaIO_4$ advanced oxidation process: response surface methodology optimization, kinetic simulation and performance enhancement

Fan Bai, Yanjiao Gao*, Yongbo Xiao, Jingyi Yang, Jiaxin Chen and Jing Xiao

College of Civil Engineering and Architecture, Liaoning University of Technology, Jinzhou 121001, China

**Total 19 pages including 4 Texts, 3 Figures, and 4 Tables.**

* Corresponding author. Email address: tmgyj@lnut.edu.cn (Y. G.).

## List of Supplementary Information:

## 1 Texts



## 2 Figures



## 3 Tables

# 1 Texts

## Text S1. Materials

Sodium sulfate ($Na_2O_4S$, 99%), and sodium bicarbonate ($NaHCO_3$, 99.8%) were sourced from Shanghai Een Chemical Technology Co. Phenol ($C_6H_6O$, 99%) was obtained from Shanghai Aladdin Biochemical Technology Co. Sodium chloride (NaCl, 99%), sodium carbonate ($Na_2CO_3$, 99%), and sodium nitrate ($NaNO_3$, 99%) was supplied by Sinopharm Chemical Reagent Co. Sodium hydroxide (NaOH, 99%) and hydrochloric acid (HCl, 99.5%) were procured from Kunshan Jincheng Reagent Co. Tert-butanol ($C_4H_{10}O$, 99.5%), furfuryl alcohol ($C_5H_6O_2$, 95%), p-benzoquinone ($C_6H_4O_2$, 97%), sodium dihydrogen phosphate ($NaH_2PO_4$, 99.9%), and humic acid (FA ≥90%) were acquired from Shanghai McLean Biochemical Technology Co.

## Text S2. Comparative analysis of various systems for degrading RB5

As shown in Fig. S1(a), the degradation of RB5 by a single SPI system and single Cu(II) system was poor with only 6.71% and 18.63% removal in 120 minutes, respectively. This indicates that SPI has a very weak oxidizing ability on RB5 in the system without the addition of a catalyst. Compared with SPI, Cu(II) has a slightly better effect on RB5 removal, which may be due to the oxidizing or adsorbing effect of Cu(II) on RB5. However, when Cu(II) and SPI coexisted in the system, the reaction was significantly accelerated, and the removal rate of RB5 within 120 minutes could reach 92.39%. This phenomenon may be assigned to the activation of SPI by Cu(II), i.e., the Cu(II)/SPI system is capable of generating a large number of ROS with strong oxidative capacity, and these substances directly oxidize RB5.[1] Additionally, the decomposition of RB5 by Cu(II)/SPI system conformed to the pseudo-first-order kinetic model with the rate constant $k_{obs}$ = 0.0224 $min^{-1}$ and the correlation coefficient $R^2$ = 0.9906, as indicated in Fig. S1(b).

## Text S3. Influence of important parameters

### Effect of initial Cu(II) concentration on RB5 degradation

Fig. S2(a) gives the degradation efficiency of RB5 under various Cu(II) concentrations. The trends of the curves demonstrated a pronounced enhancement from 6.71% to 86.57% in RB5 removal efficiency as Cu(II) concentration elevated from 0 g $L^{-1}$ to 1 g $L^{-1}$. Kinetic studies revealed that the RB5 degradation consistently followed pseudo-first-order kinetics in varying initial Cu(II) concentrations. As presented in Table S1, the $k_{obs}$ values exhibited an upward trend as the initial Cu(II) concentration rose from 0 g $L^{-1}$ to 1 g $L^{-1}$, specifically reaching 0.0008 $min^{-1}$, 0.0125 $min^{-1}$, 0.0135 $min^{-1}$, 0.0159 $min^{-1}$, and 0.0173 $min^{-1}$. This suggests that the capacity of degrading RB5 was progressively enhanced with the increasing initial Cu(II) concentration. The underlying reason might be that a higher Cu(II) concentration augments the number of active sites on the Cu(II) surface for $IO_4^-$ activation, thereby making more ROS available to break down RB5 and consequently improving the degradation efficiency of RB5 (Eqs. S1-S2).[2] A distinct trend was observed as the Cu(II) concentration doubled from 1 g $L^{-1}$ to 2 g $L^{-1}$, where the RB5 degradation performance exhibited a marginal decline rather than enhancement, with negligible variation in the observed $k_{obs}$. This phenomenon might stem from competitive coordination chemistry, where surplus Cu(II) ions potentially formed colored metal-organic complexes with RB5 molecules (possibly azo metallated intermediates), thereby altering the reaction pathway and optical properties of the solution, ultimately affecting the apparent

decolorization efficiency.[3]

$$Cu^{2+} + IO_4^- \rightarrow Cu^{3+} + IO_3^- \quad \text{(S1)}$$

$$Cu^{2+} + IO_4^- + H_2O \rightarrow Cu^{3+} + IO_3^- + O_2^{\bullet-} + 2H^+ \quad \text{(S2)}$$

**Effect of initial SPI concentration on RB5 degradation**

The correlation between SPI dosage and RB5 decolorization efficiency demonstrates a non-monotonic behavior as illustrated in Fig. S2(b). It revealed that an initial improvement phase in RB5 decomposition succeeded by a gradual decline when SPI concentrations exceeded 50 μM, with complete degradation performance decreasing from 92.39% to 86.57% as concentrations reached 100 μM. Kinetic analysis (Table S1) confirmed pseudo-first-order reaction patterns across tested concentrations, where the observed $k_{obs}$ exhibited a similar trend-increasing 8.96-fold from 0.0025 $min^{-1}$ to 0.0224 $min^{-1}$ within the 0-50 μM SPI range, then decreasing to 0.0173 $min^{-1}$ at 100 μM. This concentration-dependent behavior is attributed to dual mechanisms: Enhanced $IO_4^-$ availability at moderate SPI levels (≤50 μM) promotes efficient radical formation ($IO_3^-$ transformation and ROS generation via Eqs. S3-S6),[2] while excessive SPI concentrations (>50 μM) likely induce radical scavenging effects. The optimal catalytic performance at 50 μM SPI corresponds to a critical balance between oxidant generation and consumption pathways within the reaction system. This could be due to the occurrence of reverse and side reactions within the advanced oxidation system, as well as the significant impact of the high initial oxidant concentration on ROS.[4-6]

$$IO_4^- + 2H^+ \rightarrow IO_3^- + H_2O \quad \text{(S3)}$$

$$O^{\bullet-}+H^{+} \rightarrow HO^{\bullet} \quad \text{(S4)}$$

$$3IO_4^{-}+2OH^{-} \rightarrow 3IO_3^{-}+2O_2^{\bullet-}+2H_2O \quad \text{(S5)}$$

$$2O_2^{\bullet-}+2H_2O \rightarrow {}^1O_2+H_2O_2+2OH^{-} \quad \text{(S6)}$$

**Effect of initial pH on RB5 degradation**

The pH of the solution plays a vital role in the Cu(II)/SPI system. The pH-dependent catalytic performance of the Cu(II)/SPI system was systematically investigated through RB5 degradation experiments across a pH spectrum from 3 to 11, as presented in Fig. S2(c). Kinetic analysis (Table S1) revealed that the degradation process followed pseudo-first-order kinetics under all tested conditions. Notably, the system exhibited severely compromised catalytic activity under strongly acidic conditions (pH 3), achieving merely 6.05% RB5 removal after 120 minutes of treatment with a corresponding $k_{obs}$ value of 0.0007 $min^{-1}$. This may be because the contaminant molecule has the same surface charge as Cu(II)/SPI, and a repulsion occurs. In general, contaminant molecules may have different surface charges at different solution pH. On the other hand, the surface properties of the oxidants and catalysts used are also highly dependent on the pH of the solution.[7] Experiments have found that the point of zero charge (pzc) of RB5 is approximately between 3-4 (3.5). When the pH value of the solution is less than pHpzc, RB5 is positively charged; When the pH of the solution is greater than pHpzc, RB5 is negatively charged. When the pH value of the solution is 3, Cu(II) and SPI are positively charged on the surface, and RB5 is also positively charged, which leads to repulsion and hinders the degradation of RB5 in the system. The RB5 degradation in weak acid (pH=5) and partial neutral (pH=6.5) environments

were 92.39% and 91.34%, respectively, higher than in strongly acidic environments (pH=3). In an alkaline environment (pH=9, 11), the removal of RB5 was reduced by 10-20% in 120 minutes compared to weak acid and partial neutral environment. This is because when the pH value of the solution is greater than 3, Cu(II) and SPI have a positive charge, and the RB5 molecule has a negative charge at this time, and the opposite charges attract each other, which can better degrade the pollutants. When the pH of the solution is too high, there will be excess $OH^-$ and Cu(II) in the solution to form a $Cu(OH)_2$ precipitate. This results in a decrease in Cu(II), insufficient activation capacity for SPI, and a decrease in the amount of ROS generated, which in turn leads to a reduction in the final removal rate.[8,9]

**Effect of initial RB5 concentration on RB5 degradation**

The degradation performance of RB5 under different initial RB5 concentrations was systematically investigated, as depicted in Fig. S2(d). Experimental results revealed that following a 120-minute treatment period, the elimination percentages showed concentration-dependent characteristics: 93.53% at 25 μM, 92.39% at 50 μM, 91.66% at 75 μM, 88.45% at 100 μM, and 79.41% when the concentration reached 150 μM. This inverse correlation between initial pollutant concentration and degradation efficiency suggests potential mass transfer limitations at elevated concentrations. This demonstrates that the degradation efficiency of the Cu(II)/SPI system on RB5 diminishes as the initial concentration of RB5 increases.

## Text S4. Mechanism analysis

Drawing upon the outcomes of the free radical quenching experiments, a more in-depth analysis of the potential degradation pathways within the system was subsequently carried out. •OH and $^1O_2$, as common ROS, exhibited a significant contribution to RB5 degradation in the system. Due to its strong oxidative property, •OH was able to non-selectively attack multiple functional groups in the RB5 molecule, leading to the rapid degradation of RB5. $^1O_2$, on the other hand, through its unique energy transfer mechanism, was able to effectively disrupt the conjugation system in the RB5 molecular structure, further promoting the decolorization and mineralization of RB5. It was shown that Cu(II) and $IO_4^-$ could form a reactive complex under acidic conditions. When the complex decomposed, Cu(II) was oxidized to Cu(III), $IO_4^-$ was reduced to $IO_3^-$, and reactive oxygen species (•O) was released. Then •O was further converted to •OH by reaction with $H_2O$. In addition, Cu(III) can react with $H_2O$ to regenerate Cu(II) with additional release of •OH (Eqs. S7-S11).[10-12]

$IO_3$•and $IO_4$•as reactive iodine species played equally important roles in the Cu(II)/PI system. These iodine species with high oxidation potentials not only directly oxidized the RB5 molecule, but also triggered a series of chain reactions by reacting with the sites of higher electron cloud density in the RB5 molecule. Part of $IO_4^-$ may decompose directly to form $IO_3$•, and the $IO_3$•$^-$ and •O generated by the reaction may further participate in the oxidation reaction (Eqn. S12).[13-15]

$$CuSO_4 \cdot 5H_2O \rightarrow Cu^{2+} + SO_4^{2-} + 5H_2O \quad \text{(S7)}$$

$$Cu^{2+} + IO_4^- + nH_2O \rightarrow [Cu(IO_4)(H_2O)n]^{2-} \quad \text{(S8)}$$

$$[Cu(IO_4)(H_2O)n]^{2-} + 2H^+ \rightarrow Cu^{3+} + IO_3^- + \bullet O + (n+1)H_2O \quad \text{(S9)}$$

$$\bullet O + H_2O \rightarrow 2 \bullet OH \quad \text{(S10)}$$

$$Cu^{3+} + H_2O \rightarrow Cu^{2+} + \bullet OH + H^+ \quad \text{(S11)}$$

$$IO_4^- \rightarrow IO_3 \bullet^- + \bullet O \quad \text{(S12)}$$

## Figures

### Fig. S1

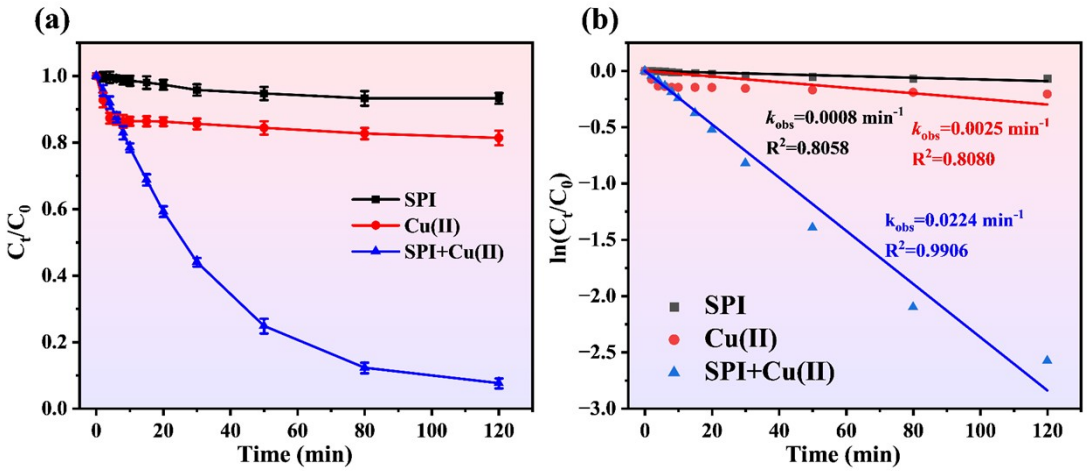


**Fig. S1** (a) Comparison plot of degradation of RB5 by systems. Conditions: [Cu(II)] = 1 g $L^{-1}$, [SPI] = 50 μM, [RB5] = 50 μM, [pH] = 6.50, (b) kinetics of RB5 degradation by different systems.

**Fig. S2**

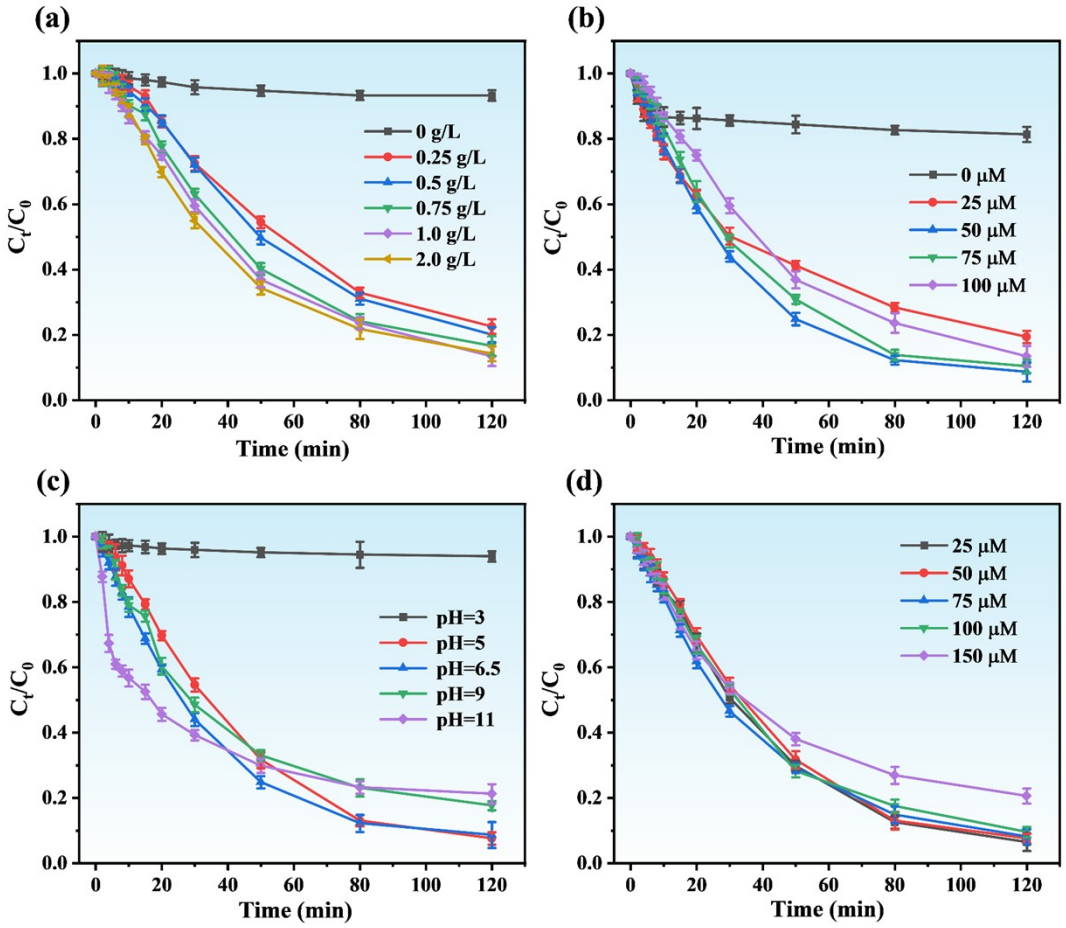


**Fig. S2** (a) Effect of Cu(II) concentration on RB5 degradation (conditions: [Cu(II)] = 0-2 g $L^{-1}$, [SPI] = 100 μM, [RB5] = 50 μM, [pH] = 6.50), (b) effect of SPI concentration on RB5 degradation (conditions: [Cu(II)] = 1 g $L^{-1}$, [SPI] = 0-100 μM, [RB5] = 50 μM, [pH] = 6.50), (c) effect of initial pH on RB5 degradation (conditions: [Cu(II)] = 1 g $L^{-1}$, [SPI] = 50 μM, [RB5] = 50 μM, [pH] = 3.00-11.00), (d) effect of the concentration of RB5 on the degradation of RB5 (conditions: [Cu(II)] = 1 g $L^{-1}$, [SPI] = 50 μM, [RB5] = 25-150 μM, [pH] = 5.00).

**Fig. S3**

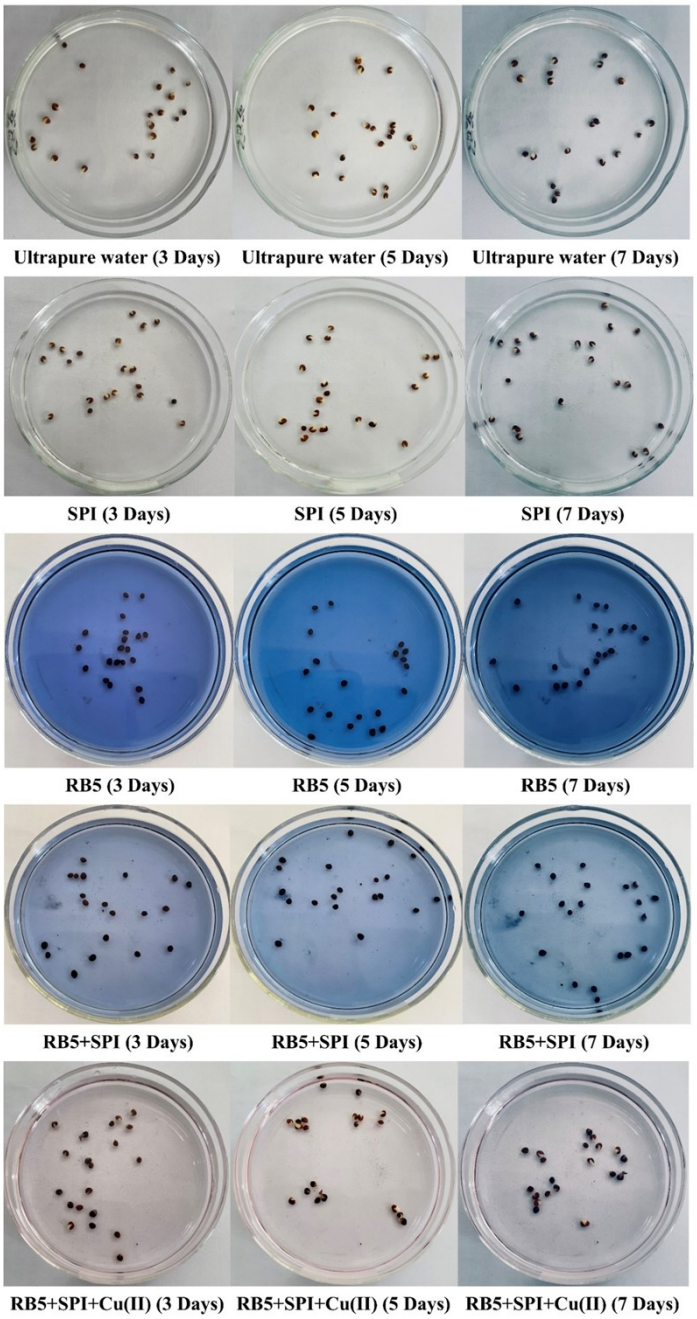


**Fig. S3** Phytotoxicity test for RB5 degradation by Cu(II)/SPI system (Ultrapure water, 1 mM of SPI, 50 μM of RB5, 1 mM of SPI+50 μM of RB5, 1 mM of SPI+50 μM of RB5+1 g $L^{-1}$ of Cu(II))

# Tables

## Table S1

**Table S1.** Kinetics of RB5 degradation by Cu(II)/SPI system under different conditions

| Cu(II) (g $L^{-1}$) | SPI (μM) | pH | RB5 (μM) | Degradation kinetic equations | $k_{obs}$ ($min^{-1}$) | $R^2$ |
|---|---|---|---|---|---|---|
| 0 | 100 | 6.5 | 50 | $-\ln(C_t/C_0)=0.0008t$ | 0.0008 | 0.9058 |
| 0.25 | 100 | 6.5 | 50 | $-\ln(C_t/C_0)=0.0125t$ | 0.0125 | 0.9859 |
| 0.5 | 100 | 6.5 | 50 | $-\ln(C_t/C_0)=0.0135t$ | 0.0135 | 0.9884 |
| 0.75 | 100 | 6.5 | 50 | $-\ln(C_t/C_0)=0.0159t$ | 0.0159 | 0.9869 |
| 1.0 | 100 | 6.5 | 50 | $-\ln(C_t/C_0)=0.0173t$ | 0.0173 | 0.9950 |
| 2.0 | 100 | 6.5 | 50 | $-\ln(C_t/C_0)=0.0176t$ | 0.0176 | 0.9878 |
| 1.0 | 0 | 6.5 | 50 | $-\ln(C_t/C_0)=0.0025t$ | 0.0025 | 0.8080 |
| 1.0 | 25 | 6.5 | 50 | $-\ln(C_t/C_0)=0.0153t$ | 0.0153 | 0.9695 |
| 1.0 | 50 | 6.5 | 50 | $-\ln(C_t/C_0)=0.0224t$ | 0.0224 | 0.9906 |
| 1.0 | 75 | 6.5 | 50 | $-\ln(C_t/C_0)=0.0211t$ | 0.0211 | 0.9839 |
| 1.0 | 50 | 3 | 50 | $-\ln(C_t/C_0)=0.0007t$ | 0.0007 | 0.8133 |
| 1.0 | 50 | 5 | 50 | $-\ln(C_t/C_0)=0.0230t$ | 0.0230 | 0.9817 |
| 1.0 | 50 | 9 | 50 | $-\ln(C_t/C_0)=0.0168t$ | 0.0168 | 0.9657 |
| 1.0 | 50 | 11 | 50 | $-\ln(C_t/C_0)=0.0172t$ | 0.0172 | 0.8326 |
| 1.0 | 50 | 5 | 25 | $-\ln(C_t/C_0)=0.0237t$ | 0.0237 | 0.9958 |
| 1.0 | 50 | 5 | 75 | $-\ln(C_t/C_0)=0.0222t$ | 0.0222 | 0.9944 |
| 1.0 | 50 | 5 | 100 | $-\ln(C_t/C_0)=0.0207t$ | 0.0207 | 0.9918 |
| 1.0 | 50 | 5 | 150 | $-\ln(C_t/C_0)=0.0151t$ | 0.0151 | 0.9725 |

**Table S2**

**Table S2.** Independent variables and levels

| Independent variables | Symbols | Levels | | |
|---|---|---|---|---|
| | | **-1** | **0** | **+1** |
| SPI (μM) | A | 25 | 50 | 75 |
| $CuSO_4$ (g $L^{-1}$) | B | 0.75 | 1 | 1.25 |
| pH | C | 4 | 5 | 6 |

**Table S3**

**Table S3.** Actual and predicted dependent variable (RB5) values for each experiment

| Run | A | B | C | RB5 removal(%) | |
|---|---|---|---|---|---|
| | | | | Actual value | Predicted value |
| 1 | 0 | 1 | -1 | 87.23 | 87.41 |
| 2 | -1 | -1 | 0 | 81.93 | 81.80 |
| 3 | 0 | 0 | 0 | 92.66 | 92.03 |
| 4 | 0 | -1 | -1 | 82.20 | 82.33 |
| 5 | 0 | 0 | 0 | 92.26 | 92.03 |
| 6 | 0 | 0 | 0 | 91.07 | 92.03 |
| 7 | 1 | 0 | 1 | 88.82 | 88.82 |
| 8 | 0 | -1 | 1 | 85.64 | 85.44 |
| 9 | 1 | 1 | 0 | 89.09 | 89.22 |
| 10 | 1 | 0 | -1 | 87.50 | 87.16 |
| 11 | 1 | -1 | 0 | 84.72 | 84.91 |
| 12 | -1 | 1 | 0 | 85.38 | 85.18 |
| 13 | 0 | 0 | 0 | 91.73 | 92.03 |
| 14 | 0 | 1 | 1 | 88.16 | 88.03 |
| 15 | 0 | 0 | 0 | 92.40 | 92.03 |
| 16 | -1 | 0 | 1 | 85.11 | 85.44 |
| 17 | -1 | 0 | -1 | 83.40 | 83.39 |

**Table S4**

**Table S4.** ANOVA test of the response function

| Source | Sum of Squares | df | Mean Square | F-value | p-value | |
|---|---|---|---|---|---|---|
| Model | 203.90 | 9 | 22.66 | 77.76 | < 0.0001 | significant |
| A-SPI | 25.57 | 1 | 25.57 | 87.76 | < 0.0001 | |
| B-$CuSO_4$ | 29.50 | 1 | 29.50 | 101.23 | < 0.0001 | |
| C-pH | 6.87 | 1 | 6.87 | 23.59 | 0.0018 | |
| AB | 0.2148 | 1 | 0.2148 | 0.7374 | 0.4189 | |
| AC | 0.0394 | 1 | 0.0394 | 0.1352 | 0.7239 | |
| BC | 1.58 | 1 | 1.58 | 5.43 | 0.0526 | |
| $A^2$ | 42.45 | 1 | 42.45 | 145.70 | < 0.0001 | |
| $B^2$ | 53.74 | 1 | 53.74 | 184.43 | < 0.0001 | |
| $C^2$ | 29.47 | 1 | 29.47 | 101.14 | < 0.0001 | |
| Residual | 2.04 | 7 | 0.2914 | | | |
| Lack of Fit | 0.4474 | 3 | 0.1491 | 0.3746 | 0.7770 | |
| Pure Error | 1.59 | 4 | 0.3980 | | | |
| Cor Total | 205.94 | 16 | | | | |

**Others: $R^2$=0.9901, Adjusted $R^2$= 0.9774, Predicted $R^2$=0.9532, Adeq Precision= 24.6958.**

## References:


**1.** A. Y. Kasim and Y. Sulfab, Kinetics and mechanism of oxidation of hexacyanoferrate (II) by periodate in acidic solutions. Evidence for copper catalysis, Inorg. *Chim. Acta*, 1977, **22**, 169-173.

**2.** R. Li, J. Wang, H. Wu, Z. Zhu and H. Guo, Periodate activation for degradation of organic contaminants: processes, performance, and mechanism, *Sep. Purif. Technol.*, 2022, **292**, 120928.

**3.** X. Huang, T. Zhu, W. Duan, S. Liang, G. Li, and W. Xiao, Comparative studies on catalytic mechanisms for natural chalcopyrite-induced Fenton oxidation: Effect of chalcopyrite type, *J. Hazard. Mater.*, 2020, **381**, 120998.

**4.** C. Lee and J. Yoon, Application of photoactivated periodate to the decolorization of reactive dye: reaction parameters and mechanism, *J. Photochem. Photobiol., A*, 2004, **165**(1-3), 35-41.

**5.** B. Neppolian, H. Jung, H. Choi, J. H. Lee and J. W. Kang, Sonolytic degradation of methyl tert-butyl ether: the role of coupled Fenton process and persulphate ion, *Water Research*, 2002, **36**(19), 4699-4708.

**6.** S. Wang, N. Zhou, S. Wu, Q. Zhang, and Z. Yang, Modeling the oxidation kinetics of sono-activated persulfate's process on the degradation of humic acid, *Ultrason. Sonochem.*, 2015, **23**, 128-134.

**7.** M. Yazdanbakhsh, H. Tavakkoli, and S. M. Hosseini, Characterization and evaluation catalytic efficiency of La0. 5Ca0. 5$NiO_3$ nanopowders in the removal of reactive blue 5 from aqueous solution, *Desalination*, 2011, **281**, 388-395.

**8.** T. Jóźwiak and U. Filipkowska, Sorption kinetics and isotherm studies of a Reactive Black 5 dye on chitosan hydrogel beads modified with various ionic and covalent cross-linking agents, *J. Environ. Chem. Eng.*, 2020, **8**(2), 103564.

**9.** M. Kosmulski, The pH-dependent surface charging, and points of zero charge. VIII. Update, Adv. Colloid Interface Sci., 2020, 275, 102064.

**10.** Y. Mao, Li. Yang, S. Liu, Y. Song, M. Luo, and Y. Guo, A theoretical study on

toluene oxidization by OH radical, *BMC Chem.*, 2024, **18**(1), 72.

**11.** Z. Rao, G. Lu, L. Chen, A. Mahmood, G. Shi, Z. Tang, X. Xie and J. Sun, Photocatalytic oxidation mechanism of Gas-Phase VOCs: Unveiling the role of holes,•OH and $O_2^{\bullet-}$, *Chemical Engineering Journal*, 2022, **430**, 132766.

**12.** M. L. Djaballah, S. Merouani, H. Bendjama and O. Hamdaoui, Development of a free radical-based kinetics model for the oxidative degradation of chlorazol black in aqueous solution using periodate photoactivated process, *J. Photochem. Photobiol.*, A, 2021, **408**, 113102.

**13.** N. Grassie, Novel types of chain reactions in polymer degradation, *Journal of Polymer Science*, 1960, **48**(150), 79-89.

**14.** T. Gu, S. He, J. Yi, Q. Liang and H. Luo, A synergistic strategy for the removal and secondary utilization of Cu (II) organic complexes in wastewater for the efficient degradation of tetracycline, *J. Environ. Chem. Eng.*, 2024, **12**(3), 112760.

**15.** Z. Huang, Z. Chu, H. Liu, T. Chen, X. Zou, F. Sun and D. Chen, Enhanced Cu-EDTA degradation with trace Cu (II) in limestone via activating PMS, S*ep. Purif. Technol.*, 2025, **358**, 130322.